

DOI: 10.1021/ic1006605



First Structurally Characterized Tricyanomanganate(III) and its Magnetic $\{Mn^{III}_{2}M^{II}_{2}\}$ Complexes $(M^{II} = Mn, Ni)$

Minao Tang,[†] Dongfeng Li,^{†,‡} Uma Prasad Mallik,[#] Jeffrey R. Withers,[#] Shari Brauer,[#] Michael R. Rhodes,[#] Rodolphe Clérac,^{⋆,§,∥} Gordon T. Yee,[⊥] Myung-Hwan Whangbo,[¶] and Stephen M. Holmes^{⋆,†,#}

[†]Department of Chemistry, University of Kentucky, Lexington, Kentucky, 40506-0055, [‡]Key Laboratory of Pesticide and Chemical Biology of Ministry of Education, College of Chemistry, Central China Normal University, 430079 Wuhan, China, [§]CNRS, UPR 8641, Centre de Recherche Paul Pascal (CRPP), 115 avenue du Dr. Albert Schweitzer, Pessac, F-33600, France, [⊥]Université de Bordeaux, UPR 8641, Pessac, F-33600, France, [⊥]Department of Chemistry, Virginia Polytechnic Institute and State University, Blacksburg, Virginia 24061, and [¶]Department of Chemistry, North Carolina State University, Raleigh, North Carolina 27695-8204. [‡]Current address: Department of Chemistry & Biochemistry, University of Missouri-St. Louis, St. Louis, Missouri 63121.

Received April 7, 2010

Treatment of tris(3-cyano-2,4-pentanedionato)manganese(III) with KTp*, followed by [NEt₄]CN affords [NEt₄][(Tp*)Mn^{III}(CN)₃] (1); subsequent treatment of 1 with divalent triflates (OTf) and 2,2′-bipyridine (bpy) affords {Mn^{III}₂M^{III}₂} complexes (M^{II} = Mn, 2; Ni, 3). Magnetic measurements show that 1-3 exhibit $S_T = 1$, 3, and 4 spin ground states, respectively.

Cyanometalates find extensive use as reagents for the rational construction of polynuclear complexes that exhibit superparamagnetism like behavior, spin crossover, and optically responsive materials. Using a synthetic strategy known as a building block approach, molecular precursors are allowed to self-assemble with intact structures into a common structural archetype. The most common units for constructing polynuclear cyanometalate complexes are those containing tripodal ligands, L, with generalized [fac-LMⁿ-(CN)_m] stoichiometry. Lea-c

Over the last five years, we have systematically investigated the use of poly(pyrazolyl)borates as platforms for tuning the magnetic and optical behavior of several structurally related

*To whom correspondence should be addressed. E-mail: holmesst@ umsl.edu (S.M.H.); clerac@crpp-bordeaux.cnrs.fr (R.C.).

tri-, tetra-, and octanuclear complexes. Tricyano- building blocks such as $[(Tp^R)Fe^{III}(CN)_3]^ (Tp^R = pzTp, Tp, Tp^*)$ exhibit substantial orbital contributions to their $S_T = \frac{1}{2}$ ground state that are crucial for engineering polynuclear complexes that exhibit slow relaxation of the magnetization (i.e., single-molecule magnets, SMMs). $\frac{1}{2}$

In oxo-carboxylate complex chemistry, high spin (S=2) manganese(III) ions are used extensively as a source of single-ion magnetic anisotropy in the design of SMMs. ^{2d} However, surprisingly few cyanomanganate analogues have been described with the best characterized example being a pentanuclear complex containing [Mn^{II}(tmphen)]²⁺ (tmphen = 3,4,7,8-tetramethyl-1,10-phenanthroline) and hexacyanomanganate(III) ions in a 3:2 ratio; ^{1b,2a} this trigonal bipyramidal complex exhibits slow dynamics below 1.8 K (for a time scale of 1 s). Surprisingly, however, no tricyano- analogues have been reported to date. In the present Communication, we describe the synthesis of the first tricyanomanganate(III) complex and its self-assembly into well-defined {Mn^{III}₂M^{II}₂} complexes.

Treatment of tris(3-cyano-2,4-pentanedionato)manganese-(III) with KTp* followed by three equivalents of [NEt₄]CN in methanol affords [NEt₄][(Tp*)Mn(CN)₃] (1) as yellow crystals.³ The infrared spectrum of 1 contains intense $\tilde{\nu}_{BH}$

^{(1) (}a) Šokol, J. J.; Hee, A. G.; Long, J. R. J. Am. Chem. Soc. 2002, 124, 7656–7657. (b) Berlinguette, C. P.; Vaughn, D.; Cañada-Vilalta, C.; Galán-Mascarós, J. R.; Dunbar, K. R. Angew. Chem., Int. Ed. 2003, 43, 1606–1608. (c) Schelter, E. J.; Prosvirin, A. V.; Dunbar, K. R. J. Am. Chem. Soc. 2004, 126, 15004–15005. (d) Li, D.; Parkin, S.; Wang, G.; Yee, G. T.; Clérac, R.; Wernsdorfer, W.; Holmes, S. M. J. Am. Chem. Soc. 2006, 128, 4214–4215. (e) Li, D.; Parkin, S.; Wang, G.; Yee, G. T.; Prosvirin, A. V.; Holmes, S. M. Inorg. Chem. 2005, 44, 4903–4905. (f) Li, D.; Clérac, R.; Parkin, S.; Wang, G.; Yee, G. T.; Holmes, S. M. Inorg. Chem. 2006, 45, 4307–4309. (g) Kim, J.; Han, S.; Cho, I.-K.; Chi, K. Y.; Heu, M.; Yoon, S.; Suh, B. J. Polyhedron 2004, 23, 1333–1339. (h) Wang, S.; Zuo, J.-L.; Zhou, H.-C.; Choi, H. J.; Ke, Y.; Long, J. R.; You, X.-Z. Angew. Chem., Int. Ed. 2002, 124, 7656–7657. (i) Wang, S.; Zuo, J.-L.; Zhou, H.-C.; Song, Y.; Gao, S.; You, X.-Z. Eur. J. Inorg. Chem. 2004, 3681–3687

^{(2) (}a) Funck, K. E.; Hilfiger, M. G.; Berlinguette, C. P.; Shatruk, M.; Wernsdorfer, W.; Dunbar, K. R. *Inorg. Chem.* **2009**, *48*, 3438–3452 and references cited therein. (b) Sato, O.; Tao, J.; Zhang, Y.-Z. *Angew. Chem., Int. Ed.* **2007**, *46*, 2152–2187 and references cited therein. (c) Li, D.; Clérac, R.; Roubeau, O.; Harté, E.; Mathonière, C.; Le Bris, R.; Holmes, S. M. *J. Am. Chem. Soc.* **2008**, *130*, 252–258. (d) Sessoli, R.; Gatteschi, D. *Angew. Chem., Int. Ed.* **2003**, *42*, 268–297.

^{(3) (}a) See the Supporting Information. (b) Crystal data for 1: $C_{26}H_{42}$ -BMnN₁₀, $P3_2$, Z=3, a=9.8102(1) Å, b=9.8102(1) Å, c=26.2483(4) Ä, V=2187.70(5) Å 3 , R1 = 0.0427, wR2 = 0.0800. Crystal data for 2: $C_{78}H_{78}B_2Mn_4N_{26}O_7S_2$, $P\overline{1}$, Z=2, a=13.431(1) Å, b=18.332(2) Å, c=19.943(2) Å, $\alpha=88.878(5)^\circ$, $\beta=89.742(5)^\circ$, $\gamma=74.204(5)^\circ$, V=4724.1(8) Å 3 , R1 = 0.0977, wR2 = 0.1886.

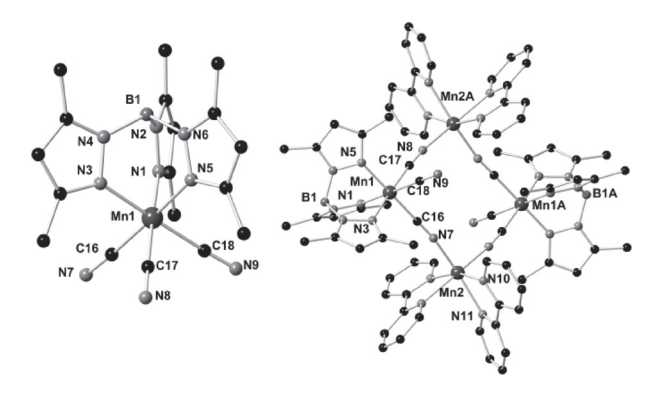


Figure 1. X-ray structures of 1 (left) and 2 (right). All cations, anions, lattice solvents, and hydrogen atoms are eliminated for clarity.

and $\tilde{\nu}_{\rm CN}$ stretches [2552 and 2113 cm $^{-1}$] that are shifted to higher energies relative to KTp* (2436 cm $^{-1}$) and [NEt₄]CN (2056 cm $^{-1}$), respectively. 4a,b For 1, the $\tilde{\nu}_{\rm CN}$ stretch is higher in energy than those seen for [Mn^{II}(CN)₂(bpy)₂] · 3H₂O (2114 cm $^{-1}$), [NEt₄]₂[Mn^{II}(CN)₄] (2120 and 2078 cm $^{-1}$), K₃[Mn^{III}(CN)₆] · H₂O (2112 and 2121 cm $^{-1}$), [NEt₄]₃[Mn^{III}(CN)₆] · H₂O (2094 cm $^{-1}$), and [PPN]₃[Mn^{III}(CN)₆] (2096 cm $^{-1}$), suggesting that charge delocalization (via π -back bonding) is less efficient. $^{3a,4b-g,5a}$

Treatment of **1** with a 1:2 ratio of Mn(OTf)₂ and bpy or [Ni(bpy)₂(OH₂)₂](OTf)₂ in acetonitrile readily affords [(Tp*)Mn^{III}(CN)₃]₂[M^{II}(bpy)₂]₂(OTf)₂·nH₂O (M^{II} = Mn, **2**; Ni, **3**). The energies of the \tilde{v}_{CN} stretches in **2** and **3** are similar to those reported for {Mn^{III}₂Mn^{II}₃} [2068–2138 cm⁻¹] and Ni^{II}₃[Mn^{III}(CN)₆]·12H₂O [2164 cm⁻¹], while intense \tilde{v}_{BH} [2551 and 2552 cm⁻¹] absorptions are comparable to those found in infrared spectra of **1**. We conclude that Mn^{III}(μ -CN)M^{II} linkages are present in **2** and **3**. 3a,4c,5a

Compound 1 crystallizes in the trigonal $P3_2$ space group. The $C_{3\nu}$ -symmetric anions have Mn–C and Mn–N distances that range between 1.976(3) and 1.985(3) Å and 2.019(2) and 2.036(2) Å, respectively, indicating that no Jahn–Teller distortions are present (Figure 1 and Supporting Information Figure S2). In 1, the average Mn–C distances [1.976(3) Å] are comparable to those in K_3 [Mn^{III}(CN)₆] [1.978(2) Å] and [PPN]₃[Mn(CN)₆] [2.020(2) Å], while the C–Mn–C angles are between 85.8(1)° [C17–Mn1–C18] and 91.7(1)° [C16–Mn1–C18]; the N–Mn–N angles are between 87.56(8)° [N3–Mn1–N5] and 89.65(9)° [N1–Mn1–N5]. 3a,5a,5b Close Tp*–Tp* methyl [3.596(3) Å] and cyanide-methyl contacts [3.452(3) Å] are also present in structures of 1 (Supporting Information Figures S3–S4). 3a

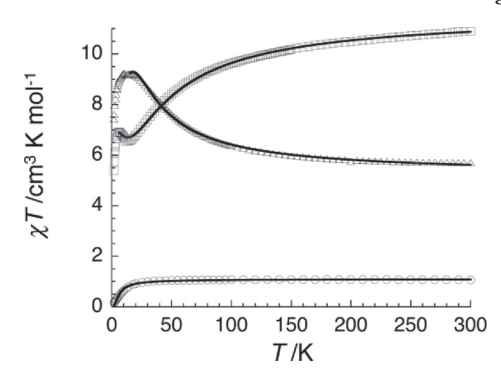


Figure 2. χT vs T plots for $\mathbf{1}$ (\bigcirc), $\mathbf{2}$ (\square), and $\mathbf{3}$ (\triangle) at $H_{\rm dc}=1000$ Oe (χ being the magnetic susceptibility defined as M/H per complex). The solid black lines are the best fit and simulations obtained (see text).

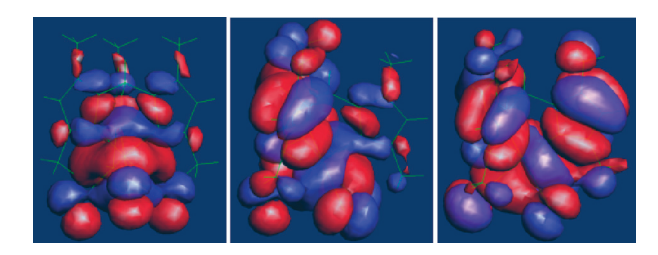


Figure 3. Shapes of the three lowest energy orbitals of **1** obtained from EHTB calculations: (left) $d(z^2)$, (middle) d(xz), and (right) d(yz) orbitals.

Crystals of **2** are found in the $P\bar{1}$ space group and its tetranuclear core consists of alternating di- and trivalent manganese ions linked by cyanides.^{3a,b} The Mn^{III} centers (Mn1 and Mn1A) contain terminal cyanides (C18–N9) that are related via inversion centers and adopt an anti-orientation relative to the {Mn^{III}₂(μ -CN)₄Mn^{II}₂} plane (Figure 1 and Supporting Information Figures S5–S7). Complex **2** is structurally related to {Fe^{III}₂MI^{II}₂} and {[V^{IV}O]₂Mn^{II}₂} analogues where a Tp* methyl projects toward the rectangular face that is opposite to the terminal cyanide.^{5c,d} The {Mn^{III}₂Mn^{II}₂} core is slightly larger than the corresponding Fe^{III} analogues due to longer average Mn1–C [1.970(6) Å] and Mn2–N [2.154(5) Å] bonds; close bpy-Tp* ring contacts [3.185(3) Å] are also present.^{3a}

At 300 K, the χT product of 1 is 1.1 cm³ K mol⁻¹, which is in good agreement with the expected value (1.0 cm³ K mol⁻¹) for a complex containing a magnetically isolated Mn^{III} ion with two unpaired electrons (Figure 2). On the other hand, the experimental χT value is far from those seen for either $[PPN]_2[Mn^{II}(CN)_4]$ or $[PPN]_3[Mn^{III}(CN)_6]$ (4.49 and 1.98 cm³ K mol⁻¹), suggesting that trivalent ions are present and that orbital contributions to the spin ground state are nearly absent in 1.3a,4d-g At low temperatures, the χT product follows Curie behavior down to 100 K and then decreases toward a minimum value of 0.15 cm³ K mol⁻¹ at 1.8 K. To reproduce this thermal behavior, an anisotropic Heisenberg Hamiltonian ($H = DS_{\text{Mn}}^2$) was utilized; the calculated values for g and D/k_B are 2.09(2) and +9.4(2) K, respectively (Figure 2 and Supporting Information Figure S8).^{3a} The surprisingly large value of D must be considered with caution as antiferromagnetic intercomplex interactions probably act to artificially enhance the estimated value. This assumption is qualitatively supported by the M versus H data (below 8 K, Supporting Information Figure S9) in that the same D value was not reproduced using an anisotropic Heisenberg model.^{3a}

^{(4) (}a) Andreades, S.; Zahnow, E. W. J. Am. Chem. Soc. 1969, 91, 4181–4190. (b) Trofimenko, S.; Long, J. R.; Nappier, T.; Shore, S. G. Inorg. Synth. 1970, 12, 99–107. (c) Smith, J. A.; Galán-Mascarós, J. R.; Clérac, R.; Sun, J.-S.; Ouyang, X.; Dunbar, K. R. Polyhedron 2001, 20, 1727–1734. (d) Buschmann, W. E.; Liable-Sands, L.; Rheingold, A. L.; Miller, J. S. Inorg. Chim. Acta 1999, 284, 175–179. (e) Manson, J. L.; Buschmann, W. E.; Miller, J. S. Inorg. Chem. 2001, 40, 1926–1935. (f) Qureshi, A. M.; Sharpe, A. G. J. Inorg. Nucl. Chem. 1968, 30, 2269–2270. (g) Buschmann, W. E.; Arif, A. M.; Miller, J. S. Angew. Chem., Int. Ed. 1998, 37, 781–783.

^{(5) (}a) Nakamoto, K. Infrared and Raman Spectra of Inorganic and Coordination Compounds, 5th ed., Part B; Wiley: New York, 1977. (b) Gupta, M. P.; Milledge, H. J.; McCarthy, A. E. Acta Crystallogr. 1974, B30, 656–661. (c) Li, D.; Parkin, S.; Wang, G.; Yee, G. T.; Holmes, S. M. Inorg. Chem. 2006, 45, 5251–5253. (d) Li, D.; Clérac, R.; Wang, G.; Yee, G. T.; Holmes, S. M. Eur. J. Inorg. Chem. 2007, 1341–1346. (e) Kambe, K. J. Phys. Soc. Jpn. 1950, 5, 48–51. (f) Li, D.; Parkin, S.; Wang, G.; Yee, G. T.; Holmes, S. M. Inorg. Chem. 2006, 45, 1951–1959. (g) Borras-Alemenar, J. J.; Clemente-Juan, J. M.; Coronado, E.; Tsukerblat, B. S. J. Comput. Chem. 2001, 22, 985–991.

Extended Hückel tight-binding (EHTB) calculations⁶ for 1 suggest that it adopts an $S_T = 1$ spin ground state, because the d(xz) and d(yz) orbitals lie close to the $d(z^2)$ orbital (225) and 267 meV above, respectively). The shapes of these orbitals (Figure 3) show that significant π -type spin density is delocalized into the Tp* and cyanide ligands. Furthermore, short $H \cdots H$ and $H \cdots NC$ -Mn contacts (ca. 2.4 and 2.7 Å) are found between adjacent [(Tp*)Mn(CN)₃] anions in 1. Below ca. 20 K these short contacts may allow for intercomplex antiferromagnetic interactions that are, as suspected (vide supra), partially responsible for the low temperature behavior of the χT data seen for 1.

For **2**, the room temperature χT value, $10.9 \text{ cm}^3 \text{ K mol}^{-1}$, is close to that expected ($10.75 \text{ cm}^3 \text{ K mol}^{-1}$) for a $\{\text{Mn}^{\text{III}}_2\text{Mn}^{\text{II}}_2\}$ complex containing noninteracting Mn^{III} $[S=1, C=1.0 \text{ cm}^3 \text{ K mol}^{-1}]$ and Mn^{II} $[S=5/_2, C=4.275 \text{ cm}^3 \text{ K mol}^{-1}]$ and Mn^{II} $[S=5/_2, C=4.275 \text{ cm}^3 \text{ K mol}^{-1}]$ and Mn^{II} $[S=5/_2, C=4.275 \text{ cm}^3 \text{ K mol}^{-1}]$ 4.375 cm³ K mol⁻¹] spins (Figure 2 and Supporting Information S10). At lower temperatures the χT values slowly decrease toward a minimum of 6.5 cm³ K mol⁻¹ at 14 K and below this temperature, χT increases, reaching a maximum of 6.9 cm³ K mol⁻¹ at 6 K. This thermal behavior indicates that antiferromagnetic interactions are dominant within the tetranuclear complex between adjacent S = 1 Mn^{III} and $S = \frac{5}{2}Mn^{II}$ spins. At lower temperatures, the χT value decreases and reaches 5.2 cm³ K mol⁻¹ at 1.85 K, suggesting the presence of magnetic anisotropy and/or intercomplex antiferromagnetic interactions. On the basis of the molecular structure of 2, the magnetic data were first modeled using an isotropic spin Hamiltonian $[H = -2J(S_1 \cdot S_2 +$ $S_2 \cdot S_3 + S_3 \cdot S_4 + S_4 \cdot S_1$ (eq 1), where J is the average exchange constant in the tetranuclear unit and S_i are the spin operators for the respective manganese ions $[S_1 = S_3 = S_{Mn(III)} = 1; S_2 = S_4 = S_{Mn(II)} = \frac{5}{2}]$. See MAGPACK simulation of the experimental data above 6 K gave a rough estimation of J/k_B at -4.8(1) K with $g(Mn^{II}) = 2.10(2)$ and $g(Mn^{III}) = 1.98(2)$ (Figure 2 and Supporting Information Figure S10), and this simple model leads to an energy difference between the $S_T = 3$ ground and $S_T = 2$ first excited states of ca. 19.2 K. Attempts to model the magnetic data with more parameters such as magnetic anisotropic or/ and intercomplex interactions were not able to improve significantly the fit of the experimental data below 6 K. The M versus H data support an $S_T = 3$ ground state for 2 as the magnetization is almost saturated at 7 T and 1.8 K and reaches 6.3 $\mu_{\rm B}$ (Supporting Information Figure S11). ^{3a} Additionally, 2 does not exhibit slow relaxation of its magnetization above 1.8 K, as judged from the lack of hysteresis in the M versus H (Supporting Information Figure S10) and frequency-independent ac susceptibility data in stark contrast to many reports on $S = 2 \text{ Mn}^{\text{III}}$ -based SMMs. We infer that the tricyanomanganate(III) ions do not bring enough magnetic anisotropy to complex 2 for the observation of SMM behavior.

The χT product at 300 K of 3 is equal to 5.4 cm³ K mol⁻¹ (Figure 2 and Supporting Information Figure S12). This value is greater than the value anticipated for isolated MnIII and Ni^{II} spins (4 cm³ K mol⁻¹ with g = 2.0). With decreasing temperature, the experimental χT product increases monotonically approaching a maximum of 9.2 cm³ K mol⁻¹ at 14 K.

The large room temperature χT product and its thermal behavior indicate that ferromagnetic interactions are present in 3. Below 14 K, the χT values decrease toward a minimum of 7.4 cm³ K mol⁻¹ at 1.85 K (Figure 2),^{3a} suggesting that additional antiferromagnetic intercomplex interactions or/ and magnetic anisotropy are present.

The magnetic data for 3 were also modeled using the Heisenberg Hamiltonian given in eq 1 with $S_i = S_{Mn(III)} =$ $S_{\text{Ni(II)}} = 1$. The susceptibility was derived from application of the van Vleck equation to the Kambe vector coupling method. 5e,f The data fitted well to ca. 25 K with $J/k_{\rm B}$ = +6.8(5) K, and g = 2.3(1). Alternative models have been tried and additional intercomplex interactions treated in terms of the mean field theory were added to the Heisenberg tetranuclear model. Above 12 K, a good fit of the data is obtained and values of $J/k_{\rm B} = +9.0(2) \text{ K}, zJ'/k_{\rm B} = -0.38(5)$ K and g = 2.3(1) are found (Figure 2 and Supporting Information S12);^{3a} introduction of an anisotropic term, $2D(S^2_z(Ni) + S^2_z(Mn))$, into the Heisenberg Hamiltonian (eq 1) was also tried and the susceptibility was calculated using the MAGPACK program. 5g Simulations of the χT versus T data between 1.8 and 300 K have been unsuccessful, suggesting that magnetic anisotropy and intercomplex antiferromagnetic interactions are likely present in 3. Nevertheless, the χT versus T data demonstrate the presence of ferromagnetic interactions between S=1 Mn^{III} and S=1 Ni^{II} spins suggesting that 3 exhibits an $S_T = 4$ ground state. At 1.8 K and $H_{\rm dc} = 7$ T, the magnetization value (7.1 $\mu_{\rm B}$) approaches that expected for an $S_T = 4$ ground state (8 μ_B) (Supporting Information Figure S13). Evidence for slow relaxation of the magnetization in 3 was absent in the M versus H and ac susceptibility data above 1.8 K, suggesting misalignment of anisotropy tensors is operative in 3.^{3a}

In summary we have described the preparation, crystal structures, and magnetic properties of a new paramagnetic tricyanomanganate(III) and two of its tetranuclear {Mn^{III}₂M^{II}₂} complexes. We have shown that the [(Tp*)Mn^{III}(CN)₃] unit possesses an $S_{\rm T}=1$ spin state that antiferromagnetically and ferromagnetically interacts with $S=\frac{5}{2}$ Mn^{II} and S=1 Ni^{II} spin centers, respectively. While slow dynamics are seen for Fe^{III} analogues of **3**, [(Tp*)Fe^{III}(CN)₃]₂[Ni^{II}(bpy)₂]₂[OTf]₂·2H₂O, ^{5d} the weaker magnetic anisotropy of the [(Tp*)Mn^{III}(CN)₃] unit leads to $S_T = 3$ and $S_T = 4$ complexes without SMM properties.

Acknowledgment. S.M.H. gratefully acknowledges the NSF (CAREER, CHE-0914935) and the University of Missouri-St. Louis for financial support. G.T.Y. acknowledges Virginia Tech and the NSF (CHE-023488) for partial support for the purchase of a Quantum Design magnetometer. M.H.W. acknowledges the U.S. DOE (DE-FG02-86ER45259). R.C. thanks the University of Bordeaux, the ANR (NT09 469563, AC-MAGnets), the Région Aquitaine, the GIS Advanced Materials in Aquitaine (COMET Project), MAGMANet (NMP3-CT-2005-515767), and the CNRS (PICS No. 4659) for support.

Supporting Information Available: Synthetic details ([NEt₄]₃- $[Mn(CN)_6]$, $[Mn(CN)_6]$, $[Mn(CN)_6]$, and X-ray crystallographic (CIF format, 1,2) and additional magnetic data (Figures S1–S6). This material is available free of charge via the Internet at http://pubs.acs.org.

^{(6) (}a) Calculations were carried out using the SAMOA package (http:// chvamw.chem.ncsu.edu/). (b) Hoffman, R. J. Chem. Phys. 1963, 39, 1397.